

# Machine learning-based tassel detection for time-series high throughput plant phenotyping

Eric Rodene<sup>1,2</sup>, Yufeng Ge<sup>2,3</sup>, James Schnable<sup>1,2</sup>, and Jinliang Yang<sup>1,2</sup>

<sup>1</sup>Department of Agronomy and Horticulture, University of Nebraska-Lincoln

<sup>2</sup>Center for Plant Science Innovation, University of Nebraska-Lincoln

<sup>3</sup>Department of Biological Systems Engineering, University of Nebraska-Lincoln

November 4, 2022



# Machine learning-based tassel detection for time-series high throughput plant phenotyping

Eric Rodene<sup>a,b</sup>, Yufeng Ge<sup>b,c</sup>, James Schnable<sup>a,b</sup>, Jinliang Yang<sup>a,b</sup>

<sup>a</sup>Department of Agronomy and Horticulture, University of Nebraska-Lincoln, Lincoln, NE 68583, USA

<sup>b</sup>Center for Plant Science Innovation, University of Nebraska-Lincoln, Lincoln, NE 68583, USA

<sup>c</sup>Department of Biological Systems Engineering, University of Nebraska-Lincoln, Lincoln, NE 68583, USA

**ORCID: 0000-0001-8318-8704**

## ABSTRACT

Unmanned aerial vehicle (UAV)-based imagery has become widely used in collecting agronomic traits, enabling a much greater volume of data to be generated in a time-series manner. As one of the cutting-edge imagery analysis tools, machine learning-based object detection provides automated techniques to analyze these imagery data. In our previous study, UAVs have been used to collect aerial photography for field trials of 233 diverse inbred lines, grown under different nitrogen treatments. Images were collected during different plant developmental stages throughout the growing season. This dataset of images has here been used in developing machine learning techniques to obtain automated tassel counts at the plot level through the season. To improve detection accuracy, we have developed an image segmentation method to remove non-tassel pixels and then feed these filtered images into machine learning algorithms. As a result, our method showed a significant improvement in the accuracy of maize tassel detection. This method can be used in future research to produce time-series counts of tassels at the plot level, and will allow for accurate estimates of flowering-related traits, such as the earliest detected flowering date and the duration of each plot's flowering period. This phenotypic data and the trait-associated genes provide new opportunities for crop improvement and to facilitate future plant breeding.

**Keywords:** high-throughput phenotyping, machine learning, maize tassel detection, image segmentation

## 1. INTRODUCTION

High-throughput phenotyping (HTP) refers to the use of advanced sensing, robotics, and automation to collect plant phenotypic data cost-effectively and across multiple scales [1]. In-field HTP for crop improvement allows large numbers of plants in the field trials to be analyzed quickly and, therefore, has the potential to improve breeding efficiency. Tassel or panicle detection in crops like maize and sorghum is particularly challenging. Conventional methods to manually measure these traits are both tedious and time-consuming. Automated methods of both detecting and counting tassels or panicles would allow traits related to flowering time to be quantified in detail, i.e., panicle counting in sorghum [2]. Recently, several machine learning algorithms, such as ResNet [3], YOLO [4], and Faster R-CNN [5], have been developed for tassel detection from unmanned aerial vehicle (UAV)-based photography [6, 7, 8, 9, 10].

Applying the existing algorithms for tassel detection in field study is challenging, especially for small plot field trials with hundreds of different genotypes. Because typical small plot field images tend to contain many complex effects, such as the interaction of light and shadows on the plant leaves, the presence of debris on the soil, and differences in lighting conditions, if images can be filtered to remove these elements, leaving behind primarily the pixels associated with tassels, the problem of training a machine learning detector to recognize tassels can be reduced to one more similar to simple shape recognition, which will likely improve tassel detection accuracy.

Here, leveraging our previously published UAV imagery data collected in a maize field trial [11], we developed a two-step tassel detection method to first filter the images and then apply machine learning algorithms to the filtered images for tassel detection. As compared with non-filtered approaches, the results using our methods show considerable improvement in the detection accuracy of individual tassels, and in particular accuracy of tassel counts, compared to ground truth data.

## 2. RESULTS

### 2.1 Image filtration removes non-tassel pixels

The images used in this study were UAV-based aerial photographs taken during the summer of 2019 on a maize diversity panel [11]. In total, over 112,000 plot-level images were obtained for 233 different genotypes planted under high nitrogen (N) and low N conditions, representing multiple replicates from July 7 to Sept 5. From these images, 323 plot-level images were randomly selected and manually annotated with bounding boxes for each tassel to serve as both training data, as well as to provide ground truth data for testing purposes (**Figure 1, Supplementary Data**). Images were selected from all dates from both nitrogen treatments and for each flowering and growth form of the diversity panel (tall-early, tall-late, short-early, and short-late).

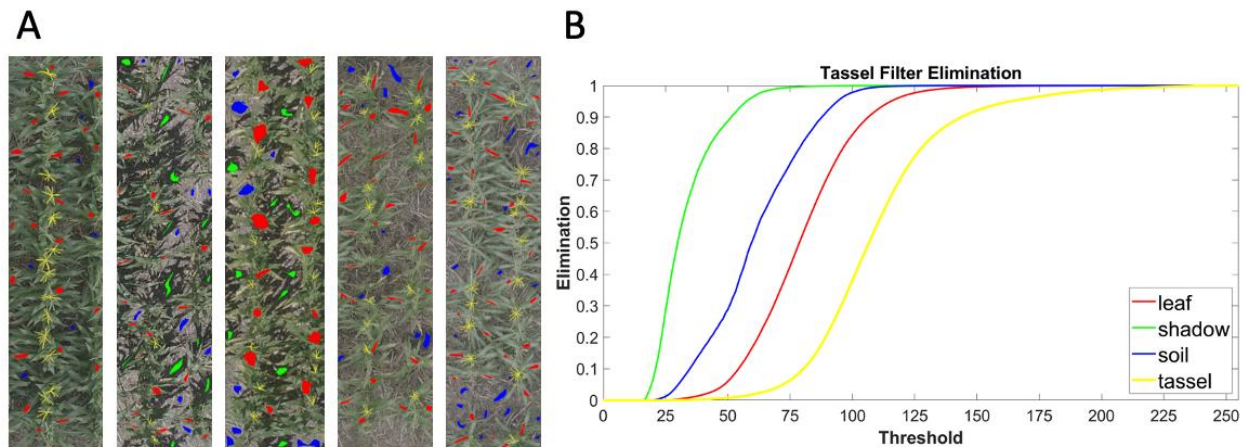


**Figure 1: Overview of the tassel filter and sampling process.** (A) Five sampled images. Images were marked for soil (blue), shadows (green), foliage (red), and tassels (yellow). (B) The elimination results of the tassel filtering. Elements (soil, shadows, foliage, and tassels) in the images are eliminated by thresholding the calculated score of the sampled pixels. As the threshold increases, greater percentages of the sampled pixels are eliminated, until 100% elimination of all sampled features is reached at the highest thresholds.

### 2.2 Filtered image improved tassel detection

The set of 323 annotated plot-level images was used to conduct randomized sample testing to evaluate the model performance. In the analysis, 80% of the image dataset (258 images) was randomly selected for the training set after being filtered at various thresholds for the different test runs (90, 95, 100, 110), while the remaining 20% (65 images) was used for the testing step on which the trained detector was applied. The filtering of the training images is a separate matter from the filtering of the images the detector is to be tested on. Early analysis indicated that filter thresholds between 90 and 110 generally produced the best results for the training images (**Figure 2**). The test images were instead filtered to varying thresholds from 0 to 255 (see **Materials & Methods**). The tassel counts at each threshold were then collected and compared to the ground truth data to calculate the prediction accuracy using correlation coefficient (i.e.,  $r^2$  values).

This allowed the  $r^2$  curves to be plotted against the filter threshold of the test images, to see what thresholds appeared to have the highest  $r^2$  values in that selection.

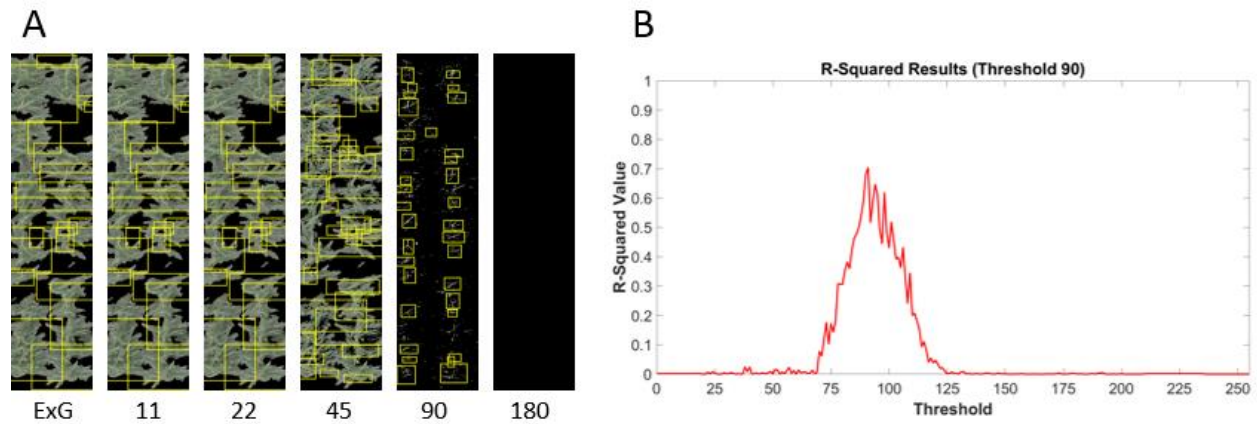


**Figure 2:  $r^2$  values at varying tassels filter thresholds.** (A) The tassels filter at thresholds of 11 to 180, based on an image pre-filtered with the Excess Green Index (far left). Bounding boxes indicate detected tassels. (B) Average  $r^2$  values calculated based on the ground truth data. The curve indicates the  $r^2$  values from using a randomized selection of images as the training data, filtered to a threshold of 90. The X-axis represents the threshold at which the sets of test images were filtered. The  $r^2$  values peak at a threshold of 91.

Leveraging the set of 323 images produced much clearer results, compared to initial tests, and also confirms that filtering of the images at thresholds between 90 and 110 generally produces the most accurate results, compared to the ground truth data (Figure 2).

### 3. MATERIALS & METHODS

#### 3.1 Procedure for image filtration

The image filtration is accomplished in two parts. The first part is to remove non-foilage elements using the Excess Green Index (ExG) [12]:

$$(1) \quad 2G^* - R^* - B^*$$

Here the values  $G^*$ ,  $R^*$ , and  $B^*$  are calculated based on the green, red, and blue channels, respectively, of each pixel of the image and dividing this value by 255, the maximum value possible in the RGB color spectrum for 8-bit integers. The calculated ExG values were further modified by rescaling them to range from 0 to 255, to make threshold selection simpler than it would be when dealing with decimal values. Previous work conducted using this same image dataset has indicated a threshold of 131 provided the most promising results for filtering of non-foilage elements for the image dataset used [11].

Once the images are filtered by the ExG, the second part of the filtering process is to remove the foliage, leaving behind only the tassels pixels. This is accomplished by using a second formula:

$$(2) \quad [2(G^* + R^*)]^2 - B^*$$

As described with the ExG above, the resulting value is then rescaled to range from 0 to 255. This formula was selected out of a variety of other possibilities by in-house tests which indicated it had the best performance with distinguishing between tassels and foliage.

The assessment of the above proposed formula was accomplished by applying it to a set of sampled images. A series of 150 plot-level images had been marked for examples of soil, shadows, foliage, and tassels (**Figure 1A**). These images were then iterated over using thresholds ranging from 0 to 255. Anytime a marked pixel was encountered, the formula was then applied to the corresponding pixel in the unmarked version of the same image. Whenever the calculated value was less than the threshold of the current iteration, it was eliminated.

It was found that the ideal filter threshold will vary substantially from image to image. However, this can be selected using cross-validation steps. Specifically, graphs are generated giving the  $r^2$  values for the selection of test images, comparing the number of tassels predicted by the detector with the ground truth observation. This resulted in a range of possible threshold values which tended to generate the highest  $r^2$  values, generally between thresholds of 90 and 110.

### **3.2 Machine learning model training**

The machine learning process was conducted using the “trainRCNNObjectDetector” function in Matlab on a detector pre-trained using the CIFAR-10 image dataset. The training settings used are very basic, with a mini-batch size of 128, an initial learning rate of 0.001, a negative overlap range from 0 to 0.3, a positive overlap range from 0.5 to 1, and conducted over 100 epochs.

## **4. DISCUSSION**

This study represents a preliminary effort to improve the tassel detection accuracy of plot-level images by using a customized filtering approach to remove most of the non-tassel pixels. Using the object-based detection methods available in Matlab, it was found that this dramatically improves the accuracy of both the predicted numbers of tassels, and also with the placement of the bounding boxes. This image segmentation can be expected to show similar results in other common object-based detection methods.

Using plot-level images for diverse maize lines, our tests using the annotated database of 323 images indicate some of the best results when the training images are pre-filtered to a threshold of 90. Likewise, we observed the highest detection accuracy when applying the trained detector to test images filtered to thresholds between 90 and 100 (**Figure 2b**).

These tassel detection methods will be used in the future to produce plot-level, time-series tassel counts using the full 2019 dataset of images. It is hoped this will uncover useful information on the flowering trends of each genotype in our study, and the effect that nitrogen treatment may have on these trends.

### **DATA AVAILABILITY STATEMENT**

The original UAV images, the clipped plot-level images, and the associated metadata used in this study have been deposited in CyVerse (10.25739/4t1v-ab64).

### **ACKNOWLEDGMENTS**

This study is supported by the Agriculture and Food Research Initiative Grant number 2019-67013-29167 and 2022-67013-36560 from the USDA National Institute of Food and Agriculture. We would also like to thank Han Tran, Daniella Tumusiime Norah, and Isabel Sigmon for their technical support in annotating the training images.

## REFERENCES

- [1] Furbank, R. T., Tester, M., “Phenomics – technologies to relieve the phenotyping bottleneck”. *Trends in Plant Science*, 16(12), 635-644 (2011).
- [2] Cai, E., Baireddy, S., Yang, C., Crawford, M., Delp, E. J., “Panicle counting in UAV images for estimating flowering time in sorghum”. arXiv:2107.07308v1 [eess.IV] (2021).
- [3] He, K., Zhang, X., Ren, S., Sun, J., “Deep Residual Learning for Image Recognition”. *Proceedings of the IEEE Conference on Computer Vision and Pattern Recognition (CVPR)*, 770-778 (2016).
- [4] Redmon, J., Divvala, S., Girshick, R., Farhadi, A., “You only look once: Unified, real-time object detection”. *Proceedings of the IEEE Conference on Computer Vision and Pattern Recognition (CVPR)*, 779-788 (2016).
- [5] Ren, S., He, K., Girshick, R., Sun, J., “Faster R-CNN: Towards real-time object detection with region proposal networks”. *Advances in Neural Information Processing Systems*, 91-99 (2015).
- [6] Lu, H., Cao, Z., Xiao, Y., Zhuang, B., Shen, C., “TasselNet: counting maize tassels in the wild via local counts regression network”. *Plant Methods*, 13:79 (2017).
- [7] Ji, M., Yang, Y., Zheng, Y., Zhu, Q., Huang, M., Guo, Y., “In-field automatic detection of maize tassels using computer vision”. *Information Processing in Agriculture*, 8, 87-95 (2019).
- [8] Liu, Y., Cen, C., Che, Y., Ke, R., Ma, Yan, Ma, Yuntao, “Detection of Maize Tassels from UAV RGB Imagery with Faster R-CNN”. *Remote Sensing*, 12(2), 338 (2020).
- [9] Zou, H., Lu, H., Li, Y., Liu, L., Cao, Z., “Maize tassels detection: a benchmark of the state of the art”. *Plant Methods*, 16:108 (2020).
- [10] Mirnezami, S. V., Srinivasan, S., Zhou, Y., Schnable, P. S., Ganapathysubramanian, B., “Detection of the Progression of Anthesis in Field-Grown Maize Tassels: A Case Study”. *Plant Phenomics* (2021).
- [11] Rodene, E., Xu, G., Palali Delen, S., Smith, C., Ge, Y., Schnable, J., Yang, J., “A UAV-based high-throughput phenotyping approach to assess time-series nitrogen responses and identify traits associated genetic components in maize”. *Plant Phenome Journal*, 5(1) (2022).
- [12] Woebbecke, D. M., Meyer, G. E., Von Bargen, K., Mortensen, D. A., “Color indices for weed identification under various soil, residue, and lighting conditions”. *Transactions of the ASAE*, 38(1), 259-269 (1995).